

1 High-throughput screening of optimal process
2 conditions using model predictive control

3

4 **Niels Krausch^a, ORCID: 0000-0003-2325-6001**

5 **Jong Woo Kim^a, ORCID: 0000-0002-4466-8745**

6 **Tilman Barz^{a,b}, ORCID: 0000-0001-7289-3627**

7 **Sergio Lucia^c, ORCID: 0000-0002-3347-5593**

8 **Sebastian Groß^d, ORCID: 0000-0002-5346-869X**

9 **Matthias C. Huber^e, ORCID: 0000-0001-9461-4414**

10 **Stefan M. Schiller^e, ORCID: 0000-0001-6864-496X**

11 **Peter Neubauer^a, ORCID: 0000-0002-1214-9713**

12 **Mariano Nicolas Cruz Bournazou^{a,f}, ORCID: 0000-0001-9461-4414**

13

14 ^aTechnische Universität Berlin, Department of Biotechnology, Chair of Bioprocess
15 Engineering, Berlin, Germany

16 ^bAIT Austrian Institute of Technology GmbH, Center for Energy, Vienna, Austria

17 ^cTechnische Universität Dortmund, Process Automation Systems, Dortmund, Germany

18 ^dWEGA Informatik (Deutschland) GmbH, Weil am Rein, Germany

19 ^eAlbert-Ludwigs-University Freiburg, Center for Biosystems Analysis, Freiburg, Germany &
20 Cluster of Excellence livMatS @ FIT, Freiburg Center for Interactive Materials and Bioinspired
21 Technologies, University of Freiburg, Freiburg, Germany

22 ^fDataHow AG, Dübendorf, Switzerland

23

24 Corresponding author: Nicolas Cruz Bournazou, n.cruz@datahow.ch

25 Keywords: high-throughput, model-predictive control, computer-aided process control

26 Running title: High-throughput screening using MPC

27 **Abstract**

28 Modern biotechnological laboratories are equipped with advanced parallel mini-bioreactor
29 facilities that can perform sophisticated cultivation strategies (e.g. fed-batch or continuous) and
30 generate significant amounts of measurement data. These systems require not only optimal
31 experimental designs that find the best conditions in very large design spaces, but also
32 algorithms that manage to operate a large number of different cultivations in parallel within a
33 well-defined and tightly constrained operating regime. Existing advanced process control
34 algorithms have to be tailored to tackle the specific issues of such facilities such as: a very
35 complex biological system, constant changes in the metabolic activity and phenotypes, shifts
36 of pH and/or temperature, and metabolic switches, e.g. by product induction, to name a few.
37 In this work we implement a model-predictive control (MPC) approach based framework to
38 demonstrate: 1) the challenges in terms of mathematical model structure, state and parameter
39 estimation, and optimization under highly nonlinear and stiff constraints in biological systems,
40 2) the adaptations required to enable its application in High Throughput Bioprocess
41 Development (HTBD), and 3) the added value of MPC implementations when operating
42 parallel mini-bioreactors aiming to maximize the biomass concentration while coping with hard
43 constrains on the Dissolved Oxygen Tension profile.

44

45 **1 Introduction**

46 The production of recombinant proteins using microbial cell factories has increased
47 dramatically over the last decades (Huang et al., 2012). However, finding optimal process
48 conditions remains a challenge, since the number of strains and possible operating conditions
49 to be tested can be very large (Neubauer et al., 2013). Miniaturization and parallelization with
50 high-throughput liquid handling stations (LHS) can significantly increase throughput and has
51 been mostly performed in microwell plates (MWP) (Knepper et al., 2014). However, cultivation
52 in MWPs has several limitations, including inhomogeneous oxygen transfer rates and limitation
53 regarding sampling, which led to a more widespread use of via mini-bioreactors (MBR) to get
54 more reliable results (Hemmerich et al., 2018). Such platforms have successfully been used

55 for protein expression studies already 15 years ago (Puskeiler et al., 2005) and computational
56 tools for design and operation of parallel experiments were integrated later on. Cruz Bournazou
57 et al. (Cruz Bournazou et al., 2017) have shown that model based re-design of dynamic
58 experiments can significantly improve information content of the experimental results for the
59 identification of parametric models. Since then, the potential of computer aided high throughput
60 cultivations were demonstrated in the context of process characterization (Sawatzki et al.,
61 2018), strain and process characterization (Anane, García, et al., 2019; Anane, Sawatzki, et
62 al., 2019; Hemmerich et al., 2019) or conditional screening of mutants (Hans et al., 2020;
63 Hemmerich et al., 2019). However, a major problem with such small-scale cultivation is that
64 they do not match the conditions in large-scale bioreactors with respect to various process
65 parameters. While there are several methods that can be used for scaling, there are still major
66 differences between laboratory-scale and industrial-scale cultivations regarding
67 inhomogeneous cultivation conditions (Nadal-Rey et al., 2021; Neubauer & Junne, 2016).
68 Hence, it is essential to ensure that the process behavior and the conclusions drawn from it
69 are as close as possible to the actual process, i.e. also reflect the conditions on a larger scale.
70 In particular, the control of the substrate feeding offers a simple way to mirror certain
71 heterogeneous process conditions. E.g. bolus feeding with pulses has shown to be an easy
72 yet powerful approach to model the effect of inhomogeneous mixing in large-scale bioreactors
73 (Anane, Sawatzki, et al., 2019). An important drawback is still the fact that due to the discrete
74 pulse-based feeding of substrate combined with significant sensor delays, it is difficult to
75 maintain the fastest modes within the desired process constrains. The dissolved oxygen
76 tension (DOT) in cultivations with organisms with a high substrate affinity (e.g. *E. coli*) offers a
77 perfect example. Here we find a number of difficulties caused by the fast dynamics of DOT
78 governed by a large oxygen transfer coefficient (kLa), the sudden changes in the oxygen
79 uptake rate dependent on the substrate availability, and the large delay of the single use DOT
80 sensor-spots on the MBRs.

81 The operation of robotic facilities for HT conditional screening is still regarded as a major
82 challenge (Morschett et al., 2021). The current contribution builds on our previous work, where

83 we successfully implemented a framework for high-throughput cultivation with conditional
84 screening capabilities in a milliliter scale (Hans et al., 2020). Avoidance of DOT limitation is a
85 crucial part in optimal operation of such devices, since pulse-based feeding typically leads to
86 drastic stress responses and elevated levels of corresponding genes (Schweder et al., 1999)
87 as well as elevated secretion of several unwanted byproducts like acetate and reduced
88 biomass yield (Bylund et al., 1998). As already mentioned, with the pulse-based feeding
89 approach used in this study, violation of this constraint might easily happen. After applying a
90 pulse, the DOT drops sharply. Conventional controllers though, could only act after a pulse
91 had been given and a constraint violation might have already occurred. Hence, a predictive
92 control algorithms like Model Predictive Controllers (MPC) are required to avoid such
93 conditions.

94 MPC is an advanced control approach based on a dynamic model of the system which
95 computes the control inputs aiming to minimize a given cost function and satisfy predefined
96 constraints (Rawlings et al., 2017). While widely applied in engineering, MPC has only found
97 relatively few applications in bioprocess engineering (see e.g. the comprehensive review by
98 Mears et al., 2017. One of the first (linear) MPC applications was presented by Kovárova-
99 Kovar et al. to maximize product formation (Kovárová-Kovar et al., 2000). Further examples
100 exist for different cases as e.g. slow growing mammalian cells (Ashoori et al., 2009), yeast
101 (Chang et al., 2016) and microbial cultivations (Del Rio-Chanona et al., 2016; Ulonska et al.,
102 2018). Another approach is to perform set point tracking to follow a predefined trajectory
103 (Craven et al., 2014; Zhang & Lennox, 2004).

104 The main challenges for the application of linear MPC result from the high nonlinearities and
105 dynamics of biological systems (Biegler, 2010). Therefore, in recent years the application of
106 nonlinear MPC (NMPC) has become more and more prominent (Allgöwer et al., 2004). MPC
107 is a powerful approach but is limited by the accuracy of the model and by the data provided to
108 make optimal decisions. In our specific case, i.e. at the early stage of cultivation, the MPC
109 framework should be able to find an optimal feeding trajectory in real-time time despite high
110 the uncertainty on the model parameter estimates and the scarce data on the strains under

111 investigation. Hence, it is of great importance to have robust adaptive methods that can
112 perform well under these difficult conditions. A common approach is to use the counterpart of
113 MPC, namely moving horizon estimation (MHE), to estimate the parameters of the process
114 while new data is generated (Rawlings et al., 2017). Using MHE for parameter re-estimation
115 has been used for process engineering for some time and various examples can be found in
116 the literature (Hedengren & Eaton, 2017; Hernández Rodríguez et al., 2021). The reader is
117 referred to Elsheikh et al., 2021 for a comprehensive review. However, none of these
118 mentioned approaches have been applied to systems that present the difficulties mentioned
119 before.

120 We will further discuss in this contribution how we tackled several issues which are commonly
121 faced in these constrained and highly perturbed fed-batch cultivations in MBRs as (i) the
122 discontinuity of the feeding regime, i.e., the bolus type addition of glucose to the reactors; (ii)
123 the delayed response of the most important state variable, the DOT in terms of sensor delay
124 and system delay to the input, which make predictive control essential to avoid constraint
125 violation; (iii) the differences in the dynamics of the timescales of the system of differential
126 equations, particularly regarding growth of biomass and the DOT, where the time dynamics
127 differ by orders of magnitudes and thus lead to a very stiff system; (iv) the different sampling
128 frequencies (high for DOT and low for biomass, glucose, and acetate); and (v) the uncertainty
129 in the parameter values of the model, which are unknown prior to the cultivation and might be
130 only based on rough knowledge about the strains. Thus, in a limited amount of time, the MHE
131 needs to solve the highly nonlinear and non-convex parameter estimation problem with
132 sufficient accuracy for the MPC to compute inputs that guide the real process to the expected
133 results.

134 We demonstrate the feasibility and added value of such an approach with real experiments
135 aiming to find optimal process conditions for the industrial production of Elastin Like Proteins
136 (ELPs). ELPs are derived from natural tropoelastin and are promising examples of
137 biocompatible, self-assembling and flexible high-performance materials with a great potential
138 for various applications (Huber et al., 2015; Huber et al., 2022; MacEwan & Chilkoti, 2014). In

139 order to develop specific protein properties, the sequence composition and length must be
140 changed significantly (Schreiber et al., 2019). The choice of the variable amino acid(s) in the
141 repetitive pentapeptide sequence as well as the size of the protein determine the phase
142 transition temperature among other characteristics, encouraging the creation of large clone
143 libraries with different strains (Huber et al., 2014) for which optimal process conditions for
144 production are yet to be identified. Due to the diverse use of individual amino acids at the fourth
145 position of the repeating sequence and a limited set of core amino acids used (especially
146 proline and valine) the optimization of ELP production depends on multiple parameters such
147 as feed strategies and oxygen supply.

148

149 **2 Materials and Methods**

150 **2.1 High throughput bioprocess development facility**

151 Experiments were conducted on our high-throughput bioprocess development platform. The
152 platform comprises two liquid handling stations (Freedom Evo 200, Tecan, Switzerland;
153 Microlab Star, Hamilton, Switzerland), a mini bioreactor system (48 BioReactor, 2mag AG,
154 Munich, Germany) and a Synergy MX microwell plate reader (BioTek Instruments GmbH, Bad
155 Friedrichshall, Germany). The reader is referred to (Haby et al., 2019) for a detailed description
156 of the facility and sampling procedure.

157

158 **2.2 Strain and cultivation conditions**

159 All experiments were carried out with *E. coli* BL21(DE3), carrying the plasmid pET28-NMBL-
160 eGFP-TEVrec-(V₂Y)₁₅-His, expressing a recombinant fusion protein of ELP and EGFP, under
161 the isopropyl-β-D-thiogalactopyranosid (IPTG) inducible *lacUV5*-promoter. Detailed
162 information about the plasmid can be found in Huber (Huber et al., 2014) and Schreiber
163 (Schreiber et al., 2019). All chemicals were purchased from either Roth, VWR or Merck if not
164 stated otherwise. For the first preculture, 10 mL LB medium, containing 16 g L⁻¹ tryptone, 10 g
165 L⁻¹ yeast extract and 5 g L⁻¹ NaCl, were directly inoculated with 100 μL cryostock and cultured
166 in in a 125 mL Ultra Yield flask (Thomson Instrument Company, USA) sealed with an AirOtop

167 enhanced flask seal (Thomson Instrument Company, USA) for 5 h at 37°C and 200 rpm in an
 168 orbital shaker (Adolf Kühner AG, Birsfelden, Switzerland). The second pre-culture was
 169 performed with 25 mL EnPresso B (Enpresso GmbH, Berlin, Germany) medium (whose
 170 composition is the same as in the main medium used, besides the glucose polymer) with 9 U
 171 L⁻¹ Reagent A to assure constant glucose release from the polymer in a 250 mL Ultra Yield
 172 flask under the same conditions as mentioned before. This allows for continuous glucose
 173 release over time and prevents overfeeding. After 12 h, while in exponential growth phase,
 174 appropriate volumes of the pre-culture were used to inoculate the MBRs to an OD600 of 0.25.
 175 The bioreactor medium consisted as derived from (Glazyrina et al., 2010) of mineral salt
 176 medium, containing (per L): 2 g Na₂SO₄, 2.468 g (NH₄)₂SO₄, 0.5 g NH₄Cl, 14.6 g K₂HPO₄, 3.6
 177 g NaH₂PO₄ × 2 H₂O, 1 g (NH₄)₂-H-citrate and 1 mL antifoam (Antifoam 204, Sigma). Before
 178 inoculation, the medium was supplemented with 2 mL L⁻¹ trace elements solution, 2 mL L⁻¹
 179 MgSO₄ solution (1.0 M) and kanamycin to a final concentration of 50 mg L⁻¹. The trace element
 180 solution comprised (per L): 0.5 g CaCl₂ × 2 H₂O, 0.18 g ZnSO₄ × 7 H₂O, 0.1 g MnSO₄ × H₂O,
 181 20.1 g Na-EDTA, 16.7 g FeCl₃ × 6 H₂O, 0.16 g CuSO₄ × 5 H₂O, 0.18 g CoCl₂ × 6 H₂O, 0.132 g
 182 Na₂SeO₃ × 5 H₂O, 0.12 g Na₂MoO₄ × 2 H₂O, 0.725 g Ni(NO₃)₂ × 6 H₂O. The composition is
 183 also derived from (Glazyrina et al., 2010). In all bioreactor cultivations, the initial glucose
 184 concentration for the batch phase was 3 g L⁻¹. At the end of the batch phase, indicated by a
 185 sharp rise of DOT, the MHE/MPC controller was started to fit the model to recent available
 186 data and start calculating an optimal feeding regime. Feeding was performed with pulses every
 187 10 min. This feeding regime exposes the cells to a short time high glucose concentration, so
 188 that they consume a lot of oxygen, which in turn could easily lead to violation of the constraint.
 189 The pulse feed for the cultivations which were not controlled by MPC was calculated according
 190 to (1) and then integrated over the pulse duration to find the volume to be added within a single
 191 pulse.

$$F(t) = \frac{\left(\frac{\mu_{set}}{Y_{X/S}} + q_m\right) * X * V}{S_i} * exp(\mu_{set} * t) \quad (1)$$

192 Where F describes the feed rate over the time t , μ_{set} the specific growth rate, $Y_{X/S}$ the yield
 193 coefficient of glucose per biomass, q_m the glucose consumption for maintenance, S_i the
 194 glucose concentration in the feed and X as well as V respectively the biomass and volume at
 195 the end of the batch phase.

196

197 **2.3 Sampling / Analytics**

198 Throughout the cultivation, DOT and pH were measured online, using photometric sensors at
 199 the bottom of the MBRs. For the other state variables, samples were taken every 20 min from
 200 one of the replicate columns and directly inactivated with dried 2 M NaOH in 96 well plates and
 201 stored at 4°C until further analysis. After collection of 3 columns of samples, the plate was
 202 automatically transferred to the Hamilton robot for at-line analysis to measure OD600, GFP,
 203 glucose and acetate concentration. The reader is referred to (Haby et al., 2019) for a detailed
 204 description of the analysis process.

205

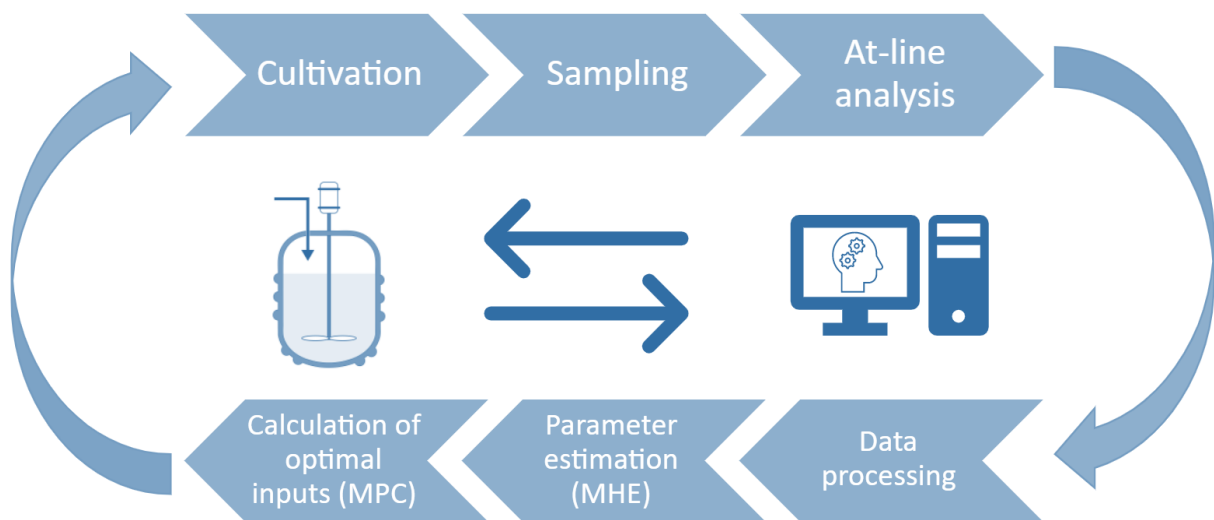
206 **2.4 MHE/MPC framework**

207 The strain was cultivated under 6 and 8 different conditions, respectively, in three replicates
 208 each consisting of a batch and an exponential fed-batch phase using a total of $n_r = 18$ mini
 209 bioreactors. Each one of the bioreactors $r \in R = \{1, \dots, n_r\}$ can be described by the nonlinear
 210 dynamics:

$$\begin{aligned} \dot{x}_r(t) &= f(x_r(t), u_r(t), \theta_r) \\ x_r(t_0) &= x_{0,r} \end{aligned} \tag{2}$$

211 The dynamic states are denoted by the vector of ODEs \dot{x}_r and include biomass, glucose, DOT,
 212 product, volume as well as acetate. The control inputs for each mini bioreactor are $u_r \in R^{n_u}$,
 213 while $\theta_r \in R^{n_\theta}$ denotes the unknown parameter vector of the reactors and cultivation conditions
 214 and $x_{0,r}$ is the initial condition for each reactor. The inputs are applied as bolus-type pulses.
 215 This leads to a highly discontinuous operation with jumps in the volume and concentrations.
 216 Thus, after each pulse, the concentrations are recalculated based on the previous

217 concentrations and the pulse volume. Time-series evolution of the denoted states can be
 218 described by a system of ordinary differential equations (ODE) and an algebraic equation, a
 219 differential-algebraic system of equations (DAE). The ODE system exhibits dynamics in very
 220 different timescales, especially regarding biomass growth and DOT, leading to a very stiff
 221 system. Since the dynamics of DOT are usually very fast compared to the other dynamics,
 222 they can be expressed in a reduced form as an algebraic equation and thereby reduce the
 223 stiffness of the system significantly (Duan et al., 2020). Since the actual DOT (DOT_a) can be
 224 only measured with a first order delay, the measured DOT (DOT_m) is also considered as a
 225 state variable, taking the response time of the sensor into account. The model has 6 differential
 226 states, 1 control input and 18 parameters in total. A complete overview about the equations of
 227 the macro kinetic growth model and the meaning of the respective parameters can be found
 228 in (Kim et al., 2021).



229
 230 **Figure 1: Flowchart of the MHE/MPC framework.** During the cultivation, samplings are taken in regular intervals,
 231 processed for at-line analysis and used for subsequent parameter estimation and MPC calculations.

232 The framework used in the study comprised of two parts: a moving horizon estimator for
 233 estimating the parameters of the model based on the recent measurements and a model
 234 predictive control part, for calculating an optimal feeding profile for each condition. An overview
 235 about the workflow is depicted in **Figure 1**. Following this procedure, the parameter set is
 236 continuously updated and used for MPC calculations. Considering the N_{MHE} last

237 measurements, the optimization problem for obtaining a new set of parameters (and in the first
 238 iteration also estimates for the initial conditions $x_{0,r}$) can be written as:

$$\min_{\theta, x_{0,r}} \frac{1}{2} \|x_{0,r} - x_{0,r,old}\|_{W_x}^2 + \frac{1}{2} \|\theta - \theta_{old}\|_{W_p}^2 + \sum_{k=0}^{N_{MHE}} \frac{1}{2} \|h(x_r(t), u_r(t), \theta) - y_{meas}(t)\|_{W_y}^2 \quad (3)$$

s.t.

$$\dot{x}_r(t) = f(x_r(t), u_r(t), \theta) \quad (4)$$

$$\theta_{min} \leq \theta \leq \theta_{max}$$

239 The estimate for the states at the initial point of the window are then denoted by $x_{0,r}$, the final
 240 optimal parameter set by θ and the previous parameter estimate is given by θ_{old} , while the
 241 final optimal parameter set is then called $\hat{\theta}$. It further considers the change in the parameters
 242 and the difference in the predicted and measured values by the squared norm. Each norm is
 243 further weighted by the weighting factors W_x, W_p, W_y . The penalty on the parameter changes
 244 assures that the parameters do not drift too much and consider their previous values.
 245 The MPC calculates optimal inputs to maximize biomass at the end of the feeding phase,
 246 considering that the DOT should not drop below a predefined threshold of 30%. A detailed
 247 description of the MPC and its mathematical formulation can be found in (Kim et al., 2021).
 248 The general problem can be written as follows:

$$\min_{u_r} -W_M X_r(t + N_{MPC}\Delta t) - W_L \sum_{k=0}^{N_{MPC}-1} X_r(t + k\Delta t) \quad (5)$$

s.t.

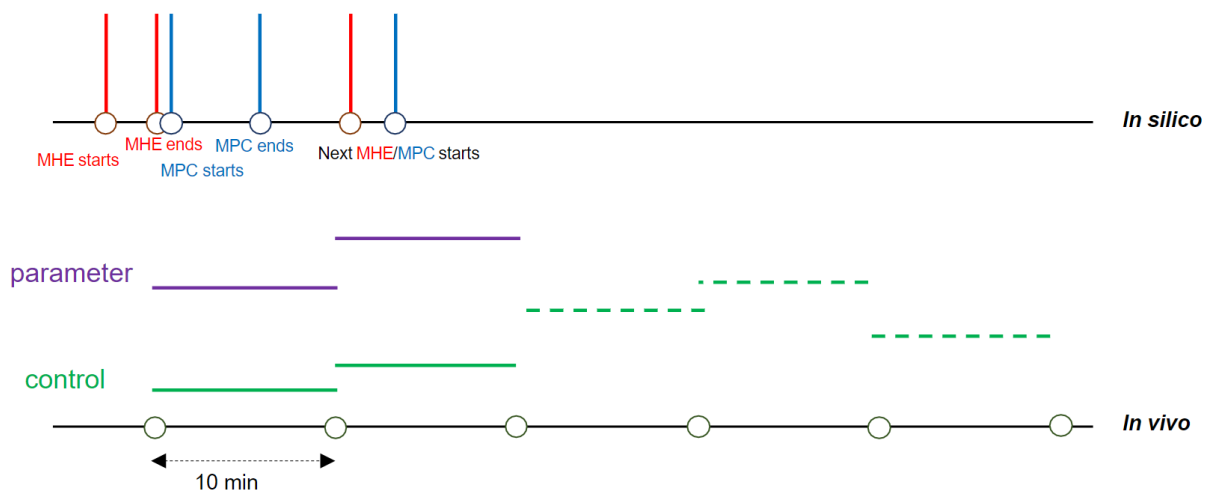
$$\dot{x}_r(t) = f(x_r(t), u_r(t), \hat{\theta}) \quad (6)$$

$$x_r(t_0) = \hat{x}_{0,r}$$

$$DOT_r(t) \geq z_{lb}, z_{lb} = 30\%, u_r(t) \geq 3$$

249 Where W_M and W_L denote the weightings for the terminal- and the stage-cost, respectively.
 250 $\hat{x}_{0,r}$ refers to the last point of the previous MHE timeframe, which is in turn the first element of
 251 the new MHE frame. In every cycle, the MHE fits the model to the recent measured values by

252 updating the parameter values. With the updated parameters, the MPC is started and
 253 calculates new inputs until the end of the feeding phase and beginning of induction. A
 254 schematic overview about the workflow is depicted in **Figure 2**.



255 **Figure 2: Overview about the MPC workflow.** Glucose pulses (the inputs) are given every 10 min as indicated by
 256 the circles. The current control inputs for each interval are represented by the green solid lines. Every 10 min, the
 257 MHE updates the model parameter (purple lines) by fitting the model to the most recent data. The updated model
 258 is used for the MPC to calculate new feeding inputs until induction. The updated inputs are represented by the
 259 dashed green lines.
 260

261
 262 The MHE/MPC framework was compared with a conventional screening approach, which
 263 tested the boundaries of the design space to identify optimal cultivation conditions as shown
 264 in **Table 1** (A-D). The values for the growth rates and the respective induction strengths used
 265 for the conventional screening approach were identified by initial screening experiments which
 266 showed that these ranges might be promising boundaries of the design space and the possible
 267 optimum is somewhere in between (data not shown).

268 **Table 1: Overview about the experimental layout.** Depicted are the 6 experimental layouts, stating if MPC was
 269 applied (+) or not (-) and in case the DOT constraint, the growth rate, and the induction strengths. The first 4 designs
 270 comprise the boundaries of the design space and are based on early screening results, while the latter 2 were
 271 controlled by MPC.

Exp. setting	MPC (DOT constraint)	μ_{set}	IPTG [mM]
A	-	0.15	0.05
B	-	0.30	0.05
C	-	0.15	2.00
D	-	0.30	2.00

E	+ (30 %)	Controlled by MPC	0.05
F	+ (30 %)	Controlled by MPC	2.00

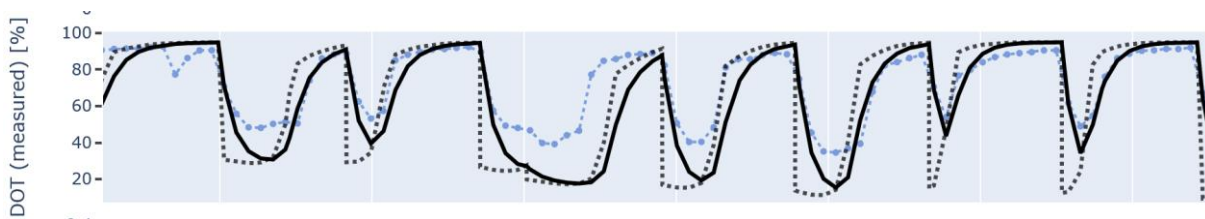
272

273 **3 Results**

274 **3.1 Coping with sensor delay**

275 The cultivation is fed via bolus feeding of glucose pulses. Even though continuous glucose
 276 release systems exist to be used on the robotic platform like EnBase (Krause et al., 2016),
 277 these systems would not reach high cell densities and cannot be controlled externally. These
 278 high concentrated glucose pulses lead to rapid oxygen uptake of the cells in the process and
 279 constraint violation, i.e., oxygen limitation, is easily possible. In such situations it is of great
 280 importance to consider the response time of the DOT sensor in the control of the process. This
 281 is especially the case when the inverse of the probe response time τ is significantly smaller
 282 than the inverse of the k_La ($\frac{1}{\tau} \ll \frac{1}{k_La}$) (Tribe et al., 1995). This is a major problem in the control
 283 of a bioprocess, where avoidance of DOT limitation is a crucial process aspect. Moreover, the
 284 DOT drops after a pulse is given, i.e., a change is applied to the system which cannot be
 285 reverted. Since the MPC framework is able to predict the actual DOT considering the sensor
 286 delay, it was possible to find an optimal feeding regime which satisfies the constraint of the
 287 actual DOT not going below 30% or 20% respectively. **Figure 3** shows the necessity to also
 288 simulate the actual DOT, since the measured DOT can be only measured with a delay and will
 289 never drop as much as the actual value. Therefore, constraint violation might be possible, even
 290 if the sensor shows that there is no oxygen limitation.

291

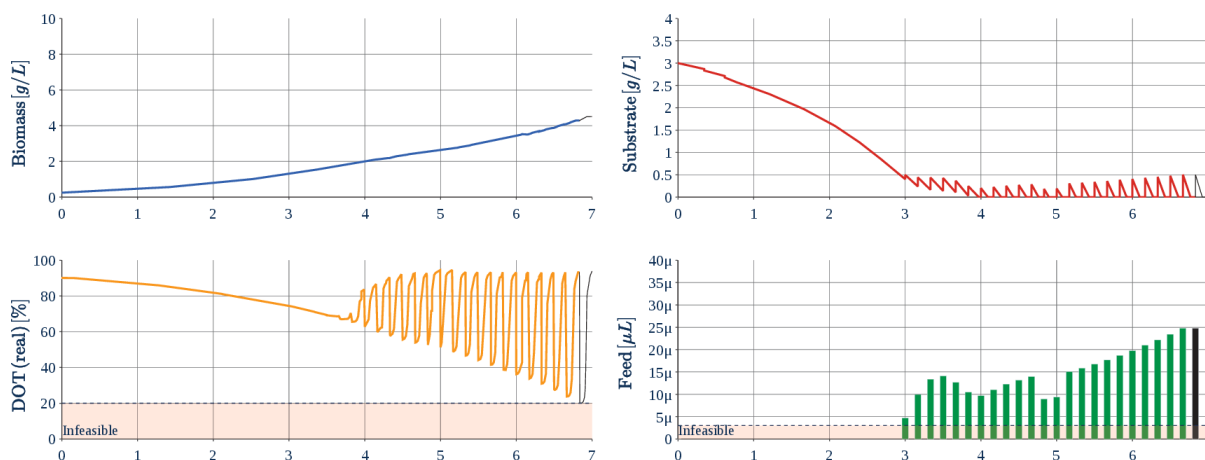


292 **Figure 3: DOT sensor delay.** Depicted are the simulated measured DOT (DOTm, solid black line) with the first
 293 order delay as well as the simulated actual DOT (DOTa, dashed line) and the real DOT measurements (blue circles
 294 and line). As can be seen in the figure, the actual DOT is declining much faster than the measured DOT and could
 295 actually violate the constraint if only the measured DOT was considered for control.

296

3.2 Identifying optimal process conditions and avoiding adverse DOT limitations

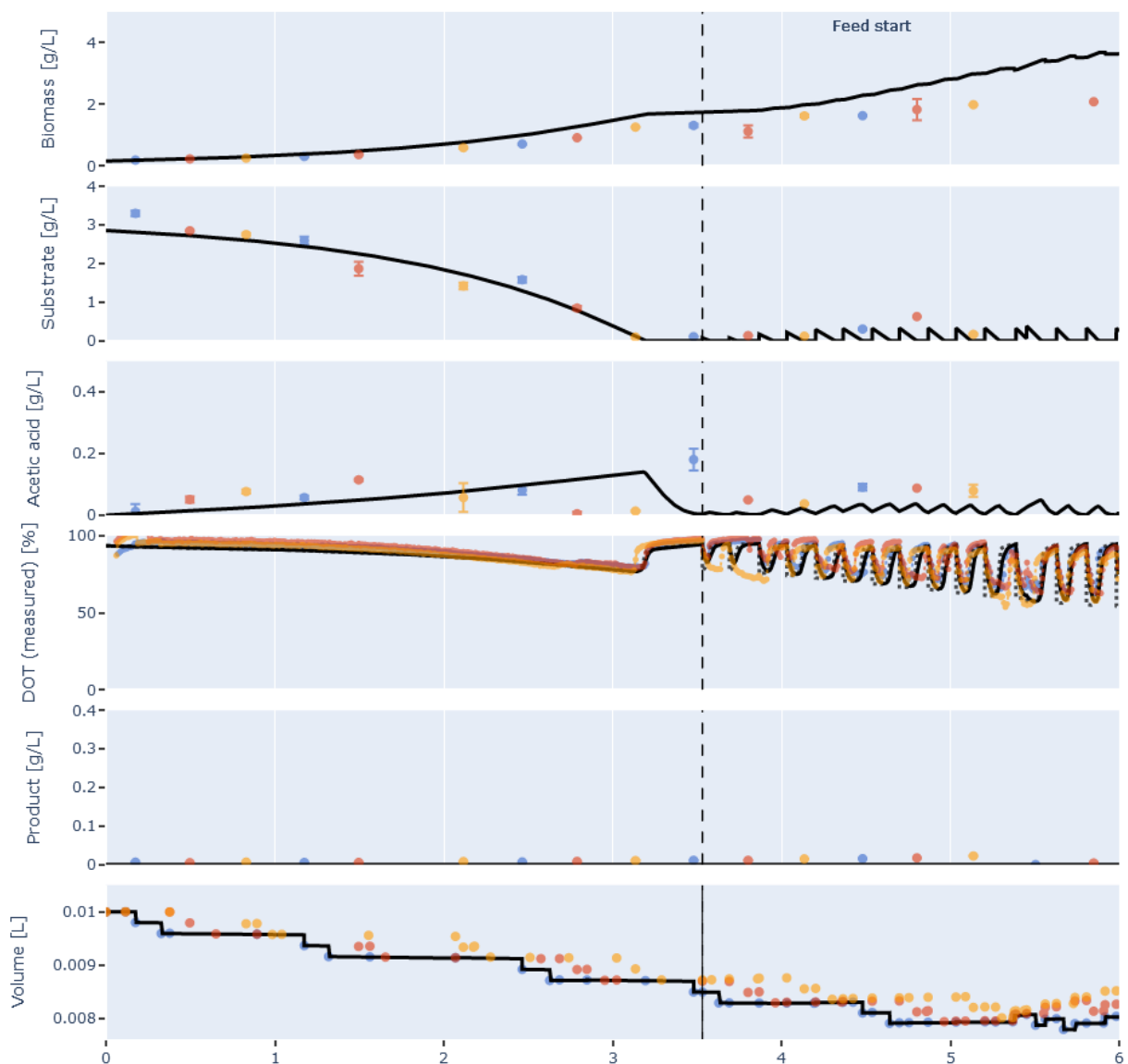
Finding optimal process conditions is a significant task in process development of a new biotechnological process. One of the critical parts is to avoid oxygen limitation in a process, since this would lead to a substantial change of the internal metabolism and lead to a significant stress response of the cells (Schweder et al., 1999). To reduce the number of experiments needed to find optimal process conditions while at the same time avoiding anoxic conditions, a HT station was combined with an innovative MPC approach. However, the MPC controller needed to cope with several restrictions in the optimization. Besides the constraint of 30 % oxygen in the reactors, the MPC had to consider that the LHS was not able to pipette less than 3 μL accurately. Under these restrictions it was possible to find a trajectory which satisfies the constraints and leads to high final biomass at the end of the feeding phase. **Figure 4** shows such a possible optimal feeding trajectory at one iteration step, indicating that the infeasible regions, that is, the regions that do not satisfy some of the constraints, are properly avoided.



310 **Figure 4: Optimal trajectory avoiding infeasible regions.** Shown is a possible trajectory calculated by the MPC
311 framework to obtain high biomass with a pulsed based feeding. Indicated are the infeasible regions as are low levels
312 of oxygen (<20%) or low pipetting volumes (< 3 μL).
313

314 The MPC framework had to calculate an optimal feeding profile based on the parameters
315 generated from the data which are measured. A critical step in the framework and for the MPC
316 to work is the estimation of reliable parameter values for the underlying model. If the values,
317 e.g. for maximum substrate uptake capacity were wrong, the MPC would also suggest a wrong
318 feeding regime, which in turn could even lead to constraint violation. The MHE updated the
319 parameter values every 10 min via fitting the model to the most recent 4 h of the process. As

320 shown in **Figure 5**, there is a good agreement between the model predictions (black solid line)
321 and the measurements from the replicate reactors. While biomass is slightly overestimated by
322 the model, there is good agreement for substrate and the measured DOT signal. Acetic acid
323 is underestimated by the model, especially in the beginning of the feeding phase, but the
324 measured values are still in a low range and the prediction error is small. Underestimating the
325 acetate could lead to wrong predictions of the substrate, since acetate is inhibiting biomass
326 growth.

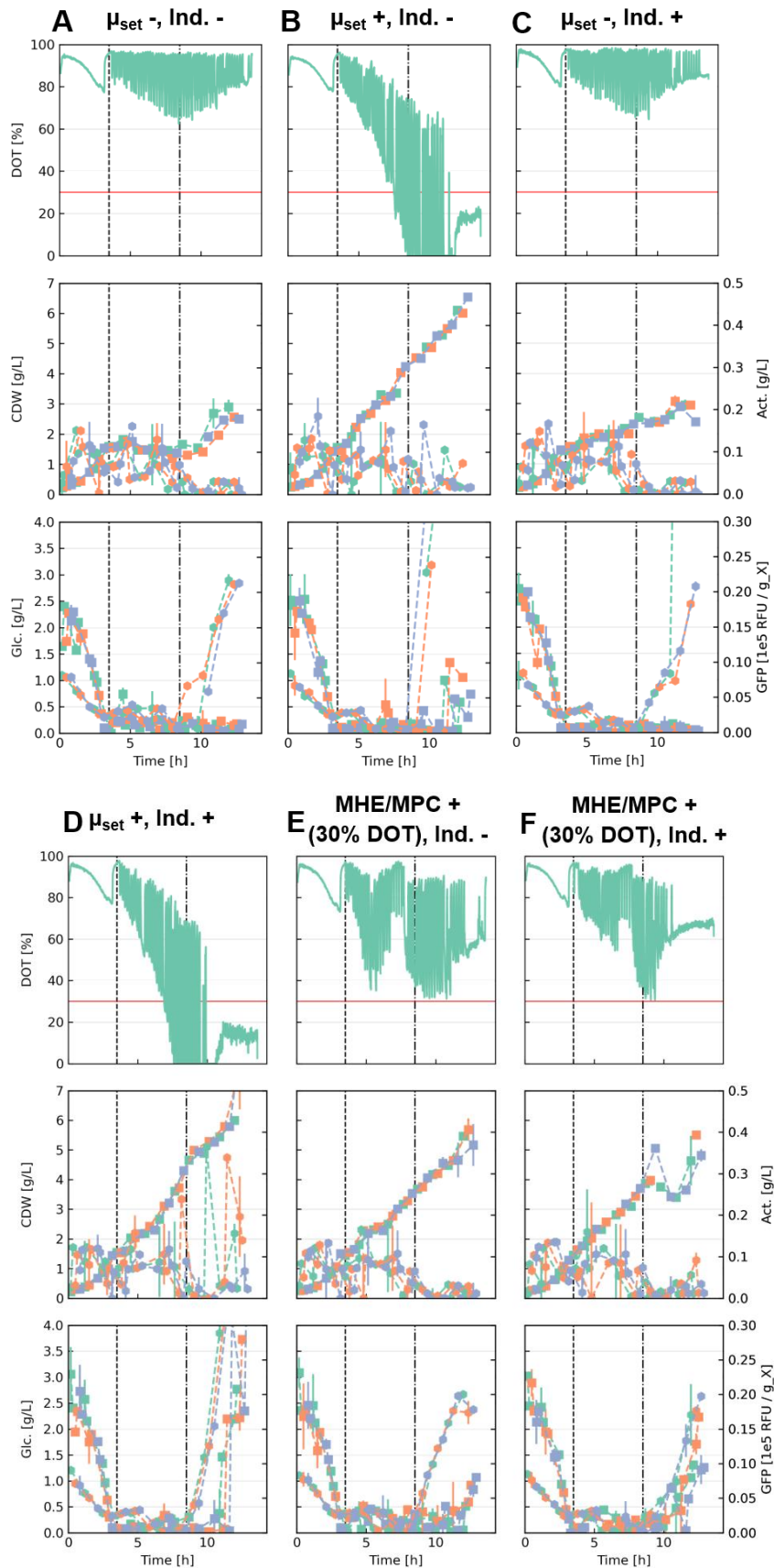


327 **Figure 5: Fitting the model to the data.** Shown are the simulated data with the most recent parameters (black
328 solid line) and measurements from 3 replicate reactors (colored dots, each color representing one of the triplicate
329 bioreactors) at a process time of around 6 h.

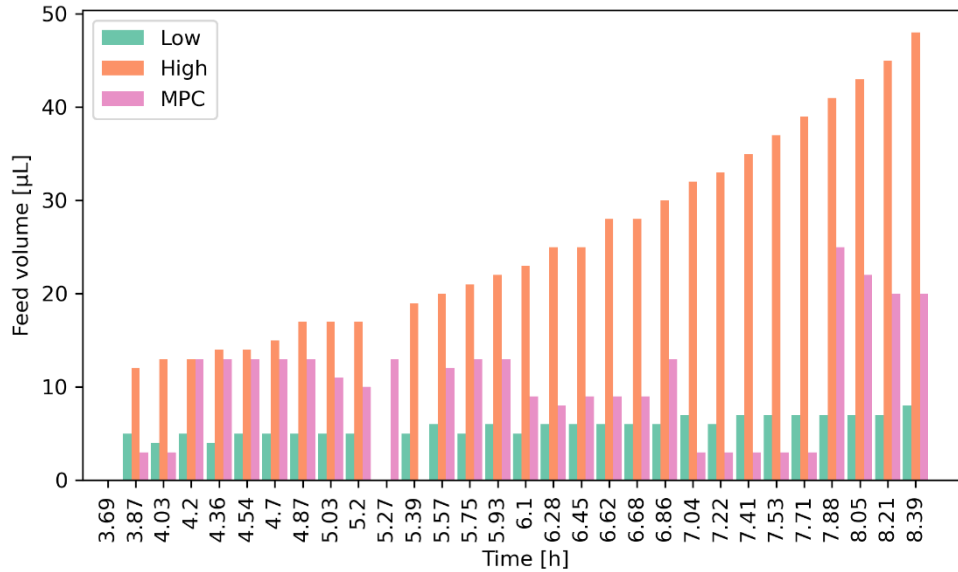
331

332 The MPC controller was able to calculate appropriate inputs for the cultivation. The results of
333 the experiments following the layout of **Table 1** are depicted in **Figure 6**. After a batch phase
334 of around 4 h, which was indicated by a sharp increase in the DOT signal, the feed was started.
335 Four reactor rows (running in triplicate) were fed with a predefined feed at a μ_{set} of 0.30 h^{-1} or
336 0.15 h^{-1} , respectively. The other two reactors were fed with individual feeds which were
337 calculated from the MPC controller and updated every 10 min. The reactors with the higher
338 predefined feed rate reached higher biomass values at the end of the process compared to
339 the reactors with the lower feed rate and therefore also higher values for the product
340 concentration as indicated by higher fluorescence as depicted in **Figure 6**. However, especially
341 after induction, the DOT signal falls below the preset threshold of 30 % in those reactors and
342 cells entered overflow metabolism, which is also indicated by glucose accumulation and higher
343 levels of acetate. Induction strength has only minor impact on the production, the cultivations
344 with the higher IPTG concentration showed slightly higher GFP levels normalized to the
345 biomass than the cultivations with lower IPTG. In the reactors which were under control of the
346 MPC framework, the biomass reached comparable levels between the high and the low
347 predefined feedrate, as also indicated by the feeding rate as shown in **Figure 7**. All reactors
348 which were operated using MPC satisfied the constraint of having oxygen levels over 30 %.
349 Glucose accumulation was only observed after induction in those reactors with the high
350 induction level and acetate kept roughly constant during the course of the cultivation. GFP
351 levels were also as high as in the cultivations with the predefined feed. As a result, the biomass
352 obtained was similar to the high μ_{set} but without violating the DOT constrains. This is an
353 increase of approx. 50 % compared to the non-controlled cultivations that stayed within bounds
354 was achieved.

355



356 **Figure 6: Results from the first cultivation.** In the figures A-D are the cultivations depicted with low (0.15) and
 357 high (0.3) feeding rate as well with low (0.02 mM) and high (2 mM) induction with IPTG. The part figures E and
 358 show the comparison of the processes which are controlled by MPC, again with the low and high induction. Depicted
 359 are the measurements for DOT, cell dry weight (squares), glucose (squares), acetate (hexagons) and normalized
 360 GFP (hexagons).



361

362 **Figure 7: Comparison of the different feeding profiles.** Shown are the different pulse volumes at each feeding
 363 time during the exponential feeding phase.

364

365 4 Discussion

366 4.1 Successful automated optimal operation of the facility

367 In this study, we extended our already existing platform for automated high-throughput
 368 bioprocess operation with an MHE/MPC framework. The implementation of MHE/MPC now
 369 enables automatic optimal operation of the high-throughput facility with only limited a priori
 370 knowledge of the process under investigation. Only with the parallel cultivation setup with
 371 automated at-line analysis of the most important state variables it is possible to generate
 372 enough data to allow a sufficient online model fitting to previously unknown strains or
 373 conditions. In contrast to the few previous examples of MPC in bioprocess engineering as
 374 mentioned in the introduction, exact parameter values do not need to be known before the
 375 experiment but are estimated by the MHE during the process. Hence, in a single run, it was
 376 possible to identify possibly optimal cultivation conditions, although some further tuning is
 377 necessary to find the optimal trajectory. Moreover, we demonstrate that the control needs to
 378 be tackled with an MPC to fulfill the DOT constraints despite the bolus feeding strategy. A
 379 classical PID controller would only react after a certain glucose pulse had already been added
 380 and a subsequent constraint violation had occurred.

381

382 **4.2 MHE/MPC guides to optimal process conditions**

383 Operating a high-throughput MBR system is a challenging task and violation of several process
384 constraints might easily happen (Hemmerich et al., 2018). This is especially true when
385 screening a new strain for optimal process conditions, where the biological parameters are
386 unknown before the experiment. The MPC controller successfully managed to maintain the
387 process within the predefined bounds. The approach was compared to a classical approach
388 with predefined feeding rates: Two different feed rates were applied to the process which are
389 often applied in bioprocesses: $\mu_{set} = 0.15 \text{ h}^{-1}$ or $\mu_{set} = 0.3 \text{ h}^{-1}$, respectively. The lower feed rate
390 did not operate the cultivation at its maximum capabilities. On the other hand, cultivating the
391 cells with the higher feed-rate led to significant oxygen limitation as can be seen in **Figure 6**.
392 An adaptive computation of the optimal profile was necessary to maximize biomass
393 concentration without violating process constraints.

394 Even though the feeding calculated with the MPC led to significantly better results than with
395 the predefined feed, the optimal feeding profile was not achieved. This is mainly due to plant-
396 model mismatches and inaccuracies of the measurements, which have great influence on the
397 simulation outcome (Anane, López C, et al., 2019). Due to the uncertainties of the parameters
398 which are currently not considered in the MPC, the actual optimal feeding rate could have been
399 higher. This problem could be tackled if for example robust MPC strategies would be applied,
400 which was not of the scope of this work, but will be applied in later stages.

401

402 **4.3 Dealing with uncertainties**

403 Uncertainties in the model parameter estimates affect the optimization of the MPC. Using an
404 approach which is less sensitive to constraint violation like Multi-Stage MPC could give better
405 results but is also computational more expensive (Lucia et al., 2013). This method could be
406 supported by using a subset selection method with sensitivity analysis or further data-driven
407 approaches like PCA (Thombre et al., 2019). However, only the combination of the MPC
408 framework with the high-throughput cultivation platform is able to generate enough data to
409 obtain good model parameters and ensure an optimal control trajectory. Due to the model

410 inaccuracies, the optimal feeding trajectory could be even better, but our study shows that
411 avoidance of oxygen limitation is possible while at the same time retaining a high growth rate.
412

413 **5 Conclusion and outlook**

414 Finding optimal experimental conditions in early bioprocess development is time consuming
415 and laborious. Even though the combination of liquid handling stations and MBR have
416 decreased the bottleneck in the screening phase, it is still not easy to find process conditions
417 which yield high biomass without violating predefined constraints which might be adverse to
418 the process under investigation. However, operating MBRs at their maximum capabilities while
419 fulfilling the constraints is essential for a fast and robust bioprocess development framework.
420 We have described how an MPC approach based on a macro-kinetic growth model can be
421 successful to maintain DOT constraints while maximizing biomass production in the
422 exponential growth phase. Hence, within a single parallel run it is possible to identify close to
423 optimal process conditions. Using an adaptive approach like MHE can alleviate this issue and
424 yield good parameters for the subsequent MPC. However, the current framework is limited by
425 the uncertainties in the parameters. More robust implementations are suggested to deal with
426 these uncertainties to ensure a sufficiently accurate parameter estimation.

427

428 **Acknowledgements**

429 We thank Felix Fiedler for his contribution to the do-mpc software and Irmgard Schäffl for the
430 early screening of the strains. We further thank labforward GmbH and DataHow AG for their
431 support within the project BioProBot. SMS & MCH gratefully acknowledge the support of the
432 BMBF (31A490 and Research Prize Next Generation of Biotechnological Processes 2014
433 Biotechnology2020+, 031A550), and the Deutsche Forschungsgemeinschaft (DFG, German
434 Research Foundation) under Germany's Excellence Strategy – EXC-2193/1 – 390951807. We
435 further gratefully acknowledge the financial support of the German Federal Ministry of
436 Education and Research (BMBF) (project no. 01QE1957C – BioProBot and 01DD20002A –

437 KIWI Biolab) and support by the German Research Foundation and the Open Access
438 Publication Fund of TU Berlin.

439

440 **Conflict of Interest**

441 The authors declare that there is no conflict of interests.

442 **References**

- 443 Allgöwer, F., Findeisen, R., & Nagy, Z. (2004). Nonlinear model predictive control: From theory to application.
444 *Journal of the Chinese Institute of Chemical Engineers*, 35(3).
- 445 Anane, E., García, Á. C., Haby, B., Hans, S., Krausch, N., Krewinkel, M., Hauptmann, P., Neubauer, P [Peter], &
446 Cruz Bournazou, M. N [Mariano Nicolas] (2019). A model-based framework for parallel scale-down fed-
447 batch cultivations in mini-bioreactors for accelerated phenotyping. *Biotechnology and Bioengineering*,
448 116(11), 2906–2918. <https://doi.org/10.1002/bit.27116>
- 449 Anane, E., López C, D. C., Barz, T [Tilman], Sin, G [Gurkan], Gernaey, K. V., Neubauer, P [Peter], & Cruz
450 Bournazou, M. N [Mariano Nicolas] (2019). Output uncertainty of dynamic growth models: Effect of
451 uncertain parameter estimates on model reliability. *Biochemical Engineering Journal*, 150, 107247.
452 <https://doi.org/10.1016/j.bej.2019.107247>
- 453 Anane, E., Sawatzki, A., Neubauer, P [Peter], & Cruz-Bournazou, M. N. (2019). Modelling concentration gradients
454 in fed-batch cultivations of E. coli - towards the flexible design of scale-down experiments. *Journal of*
455 *Chemical Technology & Biotechnology*, 94(2), 516–526. <https://doi.org/10.1002/jctb.5798>
- 456 Ashoori, A., Moshiri, B., Khaki-Sedigh, A., & Bakhtiari, M. R. (2009). Optimal control of a nonlinear fed-batch
457 fermentation process using model predictive approach. *Journal of Process Control*, 19(7), 1162–1173.
458 <https://doi.org/10.1016/j.jprocont.2009.03.006>
- 459 Biegler, L. T. (2010). *Nonlinear Programming: Concepts, Algorithms, and Applications to Chemical Processes*.
460 Society for Industrial and Applied Mathematics. <https://doi.org/10.1137/1.9780898719383>
- 461 Bylund, F., Collet, E., Enfors, S.-O [S.-O.], & Larsson, G. (1998). Substrate gradient formation in the large-scale
462 bioreactor lowers cell yield and increases by-product formation. *Bioprocess Engineering*, 18(3), 171.
463 <https://doi.org/10.1007/s004490050427>
- 464 Chang, L., Liu, X., & Henson, M. A. (2016). Nonlinear model predictive control of fed-batch fermentations using
465 dynamic flux balance models. *Journal of Process Control*, 42, 137–149.
466 <https://doi.org/10.1016/j.jprocont.2016.04.012>
- 467 Craven, S., Whelan, J., & Glennon, B. (2014). Glucose concentration control of a fed-batch mammalian cell
468 bioprocess using a nonlinear model predictive controller. *Journal of Process Control*, 24(4), 344–357.
469 <https://doi.org/10.1016/j.jprocont.2014.02.007>
- 470 Cruz Bournazou, M. N [M. N.], Barz, T [T.], Nickel, D. B., Lopez Cárdenas, D. C., Glauche, F [F.], Knepper, A [A.],
471 & Neubauer, P [P.] (2017). Online optimal experimental re-design in robotic parallel fed-batch cultivation
472 facilities. *Biotechnology and Bioengineering*, 114(3), 610–619. <https://doi.org/10.1002/bit.26192>
- 473 Del Rio-Chanona, E. A., Zhang, D., & Vassiliadis, V. S. (2016). Model-based real-time optimisation of a fed-batch
474 cyanobacterial hydrogen production process using economic model predictive control strategy. *Chemical*
475 *Engineering Science*, 142, 289–298. <https://doi.org/10.1016/j.ces.2015.11.043>

476 Duan, Z., Wilms, T., Neubauer, P [Peter], Kravaris, C., & Cruz Bournazou, M. N [Mariano Nicolas] (2020). Model
477 reduction of aerobic bioprocess models for efficient simulation. *Chemical Engineering Science*, 217,
478 115512. <https://doi.org/10.1016/j.ces.2020.115512>

479 Elsheikh, M., Hille, R., Tatulea-Codrean, A., & Krämer, S. (2021). A comparative review of multi-rate moving
480 horizon estimation schemes for bioprocess applications. *Computers & Chemical Engineering*, 146,
481 107219. <https://doi.org/10.1016/j.compchemeng.2020.107219>

482 Glazyrina, J., Materne, E.-M., Dreher, T., Storm, D., Junne, S., Adams, T., Greller, G., & Neubauer, P [Peter]
483 (2010). High cell density cultivation and recombinant protein production with *Escherichia coli* in a rocking-
484 motion-type bioreactor. *Microbial Cell Factories*, 9, 42. <https://doi.org/10.1186/1475-2859-9-42>

485 Haby, B., Hans, S., Anane, E., Sawatzki, A., Krausch, N., Neubauer, P [Peter], & Cruz Bournazou, M. N [Mariano
486 Nicolas] (2019). Integrated Robotic Mini Bioreactor Platform for Automated, Parallel Microbial Cultivation
487 With Online Data Handling and Process Control. *SLAS Technology*, 24(6), 569–582.
488 <https://doi.org/10.1177/2472630319860775>

489 Hans, S., Haby, B., Krausch, N., Barz, T [Tilman], Neubauer, P [Peter], & Cruz-Bournazou, M. N. (2020).
490 Automated Conditional Screening of Multiple *Escherichia coli* Strains in Parallel Adaptive Fed-Batch
491 Cultivations. *Bioengineering*, 7(4). <https://doi.org/10.3390/bioengineering7040145>

492 Hedengren, J. D., & Eaton, A. N. (2017). Overview of estimation methods for industrial dynamic systems.
493 *Optimization and Engineering*, 18(1), 155–178. <https://doi.org/10.1007/s11081-015-9295-9>

494 Hemmerich, J., Noack, S., Wiechert, W., & Oldiges, M. (2018). Microbioreactor Systems for Accelerated
495 Bioprocess Development. *Biotechnology Journal*, 13(4), e1700141.
496 <https://doi.org/10.1002/biot.201700141>

497 Hemmerich, J., Tenhaef, N., Steffens, C., Kappelmann, J., Weiske, M., Reich, S. J., Wiechert, W., Oldiges, M., &
498 Noack, S. (2019). Less Sacrifice, More Insight: Repeated Low-Volume Sampling of Microbioreactor
499 Cultivations Enables Accelerated Deep Phenotyping of Microbial Strain Libraries. *Biotechnology Journal*,
500 14(9), e1800428. <https://doi.org/10.1002/biot.201800428>

501 Hernández Rodríguez, T., Posch, C., Pörtner, R., & Frahm, B. (2021). Dynamic parameter estimation and
502 prediction over consecutive scales, based on moving horizon estimation: Applied to an industrial cell
503 culture seed train. *Bioprocess and Biosystems Engineering*, 44(4), 793–808.
504 <https://doi.org/10.1007/s00449-020-02488-1>

505 Huang, C.-J., Lin, H., & Yang, X. (2012). Industrial production of recombinant therapeutics in *Escherichia coli* and
506 its recent advancements. *Journal of Industrial Microbiology & Biotechnology*, 39(3), 383–399.
507 <https://doi.org/10.1007/s10295-011-1082-9>

508 Huber, M. C., Jonas, U., & Schiller, S. M. (2022). An Autonomous Chemically Fueled Artificial Protein Muscle.
509 *Advanced Intelligent Systems*, 2100189. <https://doi.org/10.1002/aisy.202100189>

510 Huber, M. C., Schreiber, A., Olshausen, P. von, Varga, B. R., Kretz, O., Joch, B., Barnert, S., Schubert, R.,
511 Eimer, S., Kele, P., & Schiller, S. M. (2015). Designer amphiphilic proteins as building blocks for the
512 intracellular formation of organelle-like compartments. *Nature Materials*, *14*(1), 125–132.
513 <https://doi.org/10.1038/NMAT4118>

514 Huber, M. C., Schreiber, A., Wild, W., Benz, K., & Schiller, S. M. (2014). Introducing a combinatorial DNA-toolbox
515 platform constituting defined protein-based biohybrid-materials. *Biomaterials*, *35*(31), 8767–8779.
516 <https://doi.org/10.1016/j.biomaterials.2014.06.048>

517 Kim, J. W., Krausch, N., Aizpuru, J., Barz, T [Tilman], Lucia, S., Neubauer, P [Peter], & Bournazou, M. N. C. (2021).
518 Model predictive control and moving horizon estimation for the pulse-based high-throughput cultivation.
519 *Preprint*.

520 Knepper, A [Andreas], Heiser, M., Glauche, F [Florian], & Neubauer, P [Peter] (2014). Robotic platform for
521 parallelized cultivation and monitoring of microbial growth parameters in microwell plates. *Journal of*
522 *Laboratory Automation*, *19*(6), 593–601. <https://doi.org/10.1177/2211068214547231>

523 Krause, M., Neubauer, A., & Neubauer, P [Peter] (2016). The fed-batch principle for the molecular biology lab:
524 Controlled nutrient diets in ready-made media improve production of recombinant proteins in *Escherichia*
525 *coli*. *Microbial Cell Factories*, *15*(1), 110. <https://doi.org/10.1186/s12934-016-0513-8>

526 Lucia, S., Finkler, T., & Engell, S. (2013). Multi-stage nonlinear model predictive control applied to a semi-batch
527 polymerization reactor under uncertainty. *Journal of Process Control*, *23*(9), 1306–1319.
528 <https://doi.org/10.1016/j.jprocont.2013.08.008>

529 MacEwan, S. R., & Chilkoti, A. (2014). Applications of elastin-like polypeptides in drug delivery. *Journal of*
530 *Controlled Release : Official Journal of the Controlled Release Society*, *190*, 314–330.
531 <https://doi.org/10.1016/j.jconrel.2014.06.028>

532 Mears, L., Stocks, S. M., Sin, G [Gürkan], & Gernaey, K. V. (2017). A review of control strategies for manipulating
533 the feed rate in fed-batch fermentation processes. *Journal of Biotechnology*, *245*, 34–46.
534 <https://doi.org/10.1016/j.jbiotec.2017.01.008>

535 Morschett, H., Tenhaef, N., Hemmerich, J., Herbst, L., Spiertz, M., Dogan, D., Wiechert, W., Noack, S., &
536 Oldiges, M. (2021). Robotic integration enables autonomous operation of laboratory scale stirred tank
537 bioreactors with model-driven process analysis. *Biotechnology and Bioengineering*, *118*(7), 2759–2769.
538 <https://doi.org/10.1002/bit.27795>

539 Nadal-Rey, G., McClure, D. D., Kavanagh, J. M., Cornelissen, S., Fletcher, D. F., & Gernaey, K. V. (2021).
540 Understanding gradients in industrial bioreactors. *Biotechnology Advances*, *46*, 107660.
541 <https://doi.org/10.1016/j.biotechadv.2020.107660>

542 Neubauer, P [Peter], Cruz, N., Glauche, F [Florian], Junne, S., Knepper, A [Andreas], & Raven, M. (2013).
543 Consistent development of bioprocesses from microliter cultures to the industrial scale. *Engineering in Life*
544 *Sciences*, 13(3), 224–238. <https://doi.org/10.1002/elsc.201200021>

545 Neubauer, P [Peter], & Junne, S. (2016). Scale-Up and Scale-Down Methodologies for Bioreactors. In C.-F.
546 Mandenius (Ed.), *Bioreactors* (Vol. 13, pp. 323–354). Wiley-VCH Verlag GmbH & Co. KGaA.
547 <https://doi.org/10.1002/9783527683369.ch11>

548 Puskeiler, R., Kaufmann, K., & Weuster-Botz, D. (2005). Development, parallelization, and automation of a gas-
549 inducing milliliter-scale bioreactor for high-throughput bioprocess design (HTBD). *Biotechnology and*
550 *Bioengineering*, 89(5), 512–523. <https://doi.org/10.1002/bit.20352>

551 Rawlings, J. B., Mayne, D. Q., & Diehl, M. (2017). *Model predictive control: Theory, computation, and design* (2nd
552 edition). Nob Hill Publishing.

553 Sawatzki, A., Hans, S., Narayanan, H., Haby, B., Krausch, N., Sokolov, M., Glauche, F [Florian], Riedel, S. L.,
554 Neubauer, P [Peter], & Cruz Bournazou, M. N [Mariano Nicolas] (2018). Accelerated Bioprocess
555 Development of Endopolygalacturonase-Production with *Saccharomyces cerevisiae* Using Multivariate
556 Prediction in a 48 Mini-Bioreactor Automated Platform. *Bioengineering (Basel, Switzerland)*, 5(4).
557 <https://doi.org/10.3390/bioengineering5040101>

558 Schreiber, A., Stühn, L. G., Huber, M. C., Geissinger, S. E., Rao, A., & Schiller, S. M. (2019). Self-Assembly
559 Toolbox of Tailored Supramolecular Architectures Based on an Amphiphilic Protein Library. *Small*, 15(30),
560 e1900163. <https://doi.org/10.1002/sml.201900163>

561 Schweder, T., Krger, E., Xu, B., Jrgen, B., Blomsten, G., Enfors, S.-O [Sven-Olof], & Hecker, M. (1999). Monitoring
562 of genes that respond to process-related stress in large-scale bioprocesses. *Biotechnology and*
563 *Bioengineering*, 65(2), 151–159. [https://doi.org/10.1002/\(SICI\)1097-0290\(19991020\)65:2<151::AID-](https://doi.org/10.1002/(SICI)1097-0290(19991020)65:2<151::AID-BIT4>3.0.CO;2-V)
564 [BIT4>3.0.CO;2-V](https://doi.org/10.1002/(SICI)1097-0290(19991020)65:2<151::AID-BIT4>3.0.CO;2-V)

565 Thombre, M., Krishnamoorthy, D., & Jäschke, J. (2019). Data-driven Online Adaptation of the Scenario-tree in
566 Multistage Model Predictive Control. *IFAC-PapersOnLine*, 52(1), 461–467.
567 <https://doi.org/10.1016/j.ifacol.2019.06.105>

568 Tribe, L. A., Briens, C. L., & Margaritis, A. (1995). Determination of the volumetric mass transfer coefficient (kLa)
569 using the dynamic "gas out-gas in" method: Analysis of errors caused by dissolved oxygen probes.
570 *Biotechnology and Bioengineering*, 46(4), 388–392. <https://doi.org/10.1002/bit.260460412>

571 Ulonska, S., Waldschitz, D., Kager, J., & Herwig, C. (2018). Model predictive control in comparison to elemental
572 balance control in an *E. coli* fed-batch. *Chemical Engineering Science*, 191, 459–467.
573 <https://doi.org/10.1016/j.ces.2018.06.074>

574 Zhang, H., & Lennox, B. (2004). Integrated condition monitoring and control of fed-batch fermentation processes.
575 *Journal of Process Control*, 14(1), 41–50. [https://doi.org/10.1016/S0959-1524\(03\)00044-1](https://doi.org/10.1016/S0959-1524(03)00044-1)